Natural Hazards
https://doi.org/10.1007/s11069-024-06590-5

ORIGINAL PAPER

Quantifying future changes of flood hazards within the Broadland catchment in the UK

Ross Gudde[1] · Yi He[1] · Ulysse Pasquier[1] · Nicole Forstenhäusler[1] · Ciar Noble[2] · Qianyu Zha[1]

Received: 31 August 2023 / Accepted: 28 March 2024

Abstract
Flooding represents the greatest natural threat to the UK, presenting severe risk to populations along coastlines and floodplains through extreme tidal surge and hydrometeorological events. Climate change is projected to significantly elevate flood risk through increased severity and frequency of occurrences, which will be exacerbated by external drivers of risk such as property development and population growth throughout floodplains. This investigation explores the entire flood hazard modelling chain, utilising the nonparametric bias correction of UKCP18 regional climate projections, the distributed HBV-TYN hydrological model and HEC-RAS hydraulic model to assess future manifestation of flood hazard within the Broadland Catchment, UK. When assessing the independent impact of extreme river discharge and storm surge events as well as the impact of a compound event of the two along a high emission scenario, exponential increases in hazard extent over time were observed. The flood extent increases from 197 km^2 in 1990 to 200 km^2 in 2030, and 208 km^2 in 2070. In parallel, exponential population exposure increases were found from 13,917 (1990) to 14,088 (2030) to 18,785 (2070). This methodology could see integration into policy-based flood risk management by use of the developed hazard modelling tool for future planning and suitability of existing infrastructure at a catchment scale.

Keywords Flood · Risk · Hazard · Exposure · Climate

1 Introduction

Flooding represents one of the natural hazards with the greatest recurrence and magnitude of incurred economic loss (Klerk et al. 2015). There are multiple sources of land inundation (e.g. storm surge and extreme precipitation) taking various forms including coastal,

✉ Yi He
yi.he@uea.ac.uk

[1] Tyndall Centre for Climate Change Research, School of Environmental Sciences, University of East Anglia, Norwich Research Park, Norwich NR4 7TJ, UK

[2] School of Environmental Sciences, University of East Anglia, Norwich Research Park, Norwich NR4 7TJ, UK

Published online: 21 April 2024

fluvial, pluvial and groundwater flooding (He et al. 2013; Klerk et al. 2015; Sayers et al. n.d). Currently, tens of millions of people are impacted by coastal flooding globally, with further damage for property and land (Adger et al. 2005; Gould et al. 2020). Development of coastal lowlands and floodplains severely increases this flood damage potential, with approximately 230 million people worldwide living in locations less than 1 m above high tide (Sayers et al. 2022). Flooding is the most significant natural threat in the UK, with upwards of 6 million properties and key infrastructure at risk from inundation (Defra 2012). This was evident in the 1953 'Big Flood' which caused 2,000 fatalities around the southern North Sea (Spencer et al. 2014) in addition to £40–50 million in damages (excluding costs of relocation and business interruption), equivalent to approximately £1 billion at today's rates (Cabinet Office 2010). Furthermore, the summer 2007 floods (Horsburgh et al. 2008), incurred an approximate cost of £3.2 billion (£2.5–3.8 billion; 2007 prices), of which £2.0 billion was insured or experienced some compensation (Chatterton et al. 2010). A more recent example is the 2013/14 winter floods, with a total economic loss estimated between £1.0-1.5 billion, with a quarter of this figure associated with residential damages (10,465 properties) (Environment Agency 2016). Inundation events are predicted to increase in severity. The third Climate Change Risk Assessment (CCRA) states that within a scenario of 2 °C warming by 2100, flooding annual losses for non-residential buildings will likely increase at rates of 27% by 2050 and 40% by 2080 and notes the figures did not consider coastal erosion (Surminski 2021). Bates et al. (2023) estimated that UK 1-in-100-year flood losses would be 6% greater for the average climate conditions of 2020 (1.1°C of warming) compared to those of 1990 (0.6°C of warming).

As a significant influencing factor on future flood impact, global mean sea level rise (SLR) of 14 cm within the 20th century (UKMMAS Community 2010) is predicted to continue with climate models projecting midlatitude SLR of 0.8–2 m by 2100 (which carries substantial uncertainty) (Pfeffer et al. 2008) that can vary regionally through glacio-isostatic rebound (Bradley et al. 2009). Ongoing SLR is driven through oceanic thermal expansion, melting of land ice (e.g. the Greenland and Antarctic ice sheets) and hydrological exchange of terrestrial land reservoirs to oceans (Oppenheimer et al. 2019).

Environmental effects from climate change are not exclusive to SLR. The increasing magnitude and frequency of extreme precipitation can lead to greater river discharge and add further stress to the coastal areas, especially if peak river flows coincide with coastal flooding (Svensson and Jones 2002). Included within the primary drivers of flooding are storm surges, which can be exacerbated within a 'compound event' (Seneviratne et al. 2012). Compound events are the temporal 'clustering' of multiple hazard events, either in close succession or coinciding, acting synergistically to produce an amplified impact. A compound event could include the simultaneous incidence of a storm surge and intense precipitation, carrying significant potential for incurring loss in low-lying coastal floodplains (Jonkman et al. 2008; Wahl et al. 2015).

The Norfolk and Suffolk Broads in East Anglia are located around or below sea level, lying immediately adjacent to the North Sea, experiencing a tidally dominated regime extending to 40–50 km inland causing significant saline intrusion (Broads Authority 2014; CH2M 2016; Pasquier et al. 2020; Environment Agency 2022). The Broadland catchment area covers approximately 3,200 km^2 with over 850,000 residents and contains thirteen major settlements, including Norwich, Great Yarmouth and Lowestoft (Broads Authority 2014). It contains an intricate network of rivers, presenting a complex system that can flood

both tidally and fluvially (Pasquier et al. 2020). The Broads have an extensive record of flooding (Mosby 1939; Spencer et al. 2015; Matless 2019); a key event being the 1953 east coast 'Big Flood', which caused 307 on-land mortalities in East Anglia from drowning and exposure (Baxter 2005). At this time, flood protection held a localised scope, whereas recently a more strategic focus has been developed, with a push for greater understanding of coastal processes and stakeholder involvement (Day et al. 2015). This has culminated in a sequence of Shoreline Management Plans (SMPs) that operate in coastal cells to strategically define coastal management into the future (Defra 2006a, 2006b). Acceptance of such plans has seen some rebuke by local populations, for example, the 2004 SMP6 proposal of abandonment of various North Norfolk cliff defences (Day et al. 2015). Therefore, greater emphasis has been cast on collaboration with stakeholders and smoothing of the phasing out of current defences via the introduction of via transitional "epochs" that provide further clarity (Defra 2006b). To reinforce these plans, the Climate Change Act 2008 brought in a requirement of more comprehensive, regular and forward-thinking assessment of flood and coastal erosion risks, where documents such as the UK Climate Change Risk Assessment are updated routinely and in-line with scientific advancements (Defra 2012). This history, and government mandate, has prompted supplementary research, for example by Norfolk County Council (2015) which reported that around 37,000 properties within Norfolk could be at risk to a 200-year hydrometeorological flood event, placing Norfolk 10th out of 152 Lead Local Flood Authorities in England in terms of flood risk. Lead Local Flood Authorities are the unitary authority or county council tasked with mitigating local flood risks in collaboration with external organisations (e.g. the Environment Agency or water and sewerage companies) (Environment Agency 2013). CH2M (2016) states that approximately 30,000 hectares of land are at risk from flooding, while 21,300 hectares are safeguarded by existing flood defences. Sea defences are at the forefront of protecting the Broads from flooding, where a 'hold the line' strategy has been implemented with 13 km of coastal defences from Eccles-On-Sea to Winterton-On-Sea commissioned by the 2012 Kelling to Lowestoft SMP (Environment Agency 2012; Hooton 2015). The major flood defence of the Broads comprises of over 240 km of earth ramparts along the catchment's major rivers, the Bure, Wensum, Waveney, Yare and Ant, alongside river channel and drainage network maintenance, protecting 24,000 hectares of prime agricultural land, 1,700 properties, 28 Sites of Specific Scientific Interest (SSSIs), and rail and road infrastructure (Environment Agency 2021). These riverine measures are managed by the Broads Authority's Broadland Rivers Catchment Flood Management Plan (Environment Agency 2009). Further management is spread throughout the catchment, with the low-elevation land segmented into 40 discrete flood compartments by high ground or flood barriers managed by local Internal Drainage Boards (CH2M 2016).

Similar studies into the potential dynamics of severe inundation within this region are scarce. Hazard has seen investigation within the Broadland region, where studies include Thumerer et al. (2000) and Mokrech et al. (2012), assess the east coast of England. Thumerer et al. (2000) offers flood impact assessment into potential economic damage for a range of land classes, describing significant exposure potential to commercial and industrial land use classes; while Mokrech et al. (2012) investigated future exposure along various socio-economic pathways, predicting significant rise in flood exposure because of projected expansion of new residential and non-residential properties into the coastal floodplain. Further investigation is presented by Pasquier et al. (2018) utilising state-of-the-art modelling

techniques including 1D-2D hydraulic modelling, a method which requires further exploration in a variety of environments, an example being Webster et al. (2014). More recently, Pasquier (2020) refined this exploration with bias correction to projected meteorological inputs and the Revised Joint Probability Method (Environment Agency 2011) to better predict storm surges. While these have fulfilled comprehensive analysis, producing key results detailing increasing severity of extreme flood events within the Broadland catchments' future, greater resolution data is now available to enhance accuracy of predicted future inundation. These state-of-the-art methods and concepts should see further integration into a comprehensive analysis of flood hazard within a complex social ecological system such as the Broads, UK, combining techniques across these studies with the newest data available (UKCP18 convection-permitting model projections) to deliver a catchment-scale flood impact assessment framework.

This study aims to assess how flood hazard dynamics change in the Broadland catchment into the future, targeting future research and management of complex hydrological environments. Modelled scenarios determined flood hazard in baseline (1990), mid-term (2030) and long-term (2070) periods, following the UKCP18 'worst-case' Representative Concentration Pathway 8.5. Flood modelling components were derived from Pasquier (2020) and He et al. (2022) to simulate compound floods of both coastal, fluvial and a combination of these sources. The UKCP18 local projections were bias corrected as future projections to feed into the flood modelling chain (Met Office Hadley Centre 2019).

2 Data and methodology

The flood impact analysis modelling chain is displayed in Fig. 1, which displays the stages and processes involved. Originating from UKCP18 sea level rise and meteorological datasets, the methodology moves through statistical techniques such as bias correction and extreme value analysis as well as integrated hydrological and hydraulic modelling, to simulate extreme inundation events along multiple probabilistic pathways.

2.1 Study area

Five major rivers drain into the Broadland catchment. They include the Ant, Bure, Wensum, Yare and Waveney which propagate through low-lying, relatively flat floodplains of the Broads National Park towards the coastal outlets of Great Yarmouth and Lowestoft (Environment Agency 2009). Their original catchment boundaries from the NRFA do not lie immediately upstream of the Broadland catchment, and hence they were adjusted to provide upstream boundary conditions to the HEC-RAS model. The adjusted catchments' boundar-

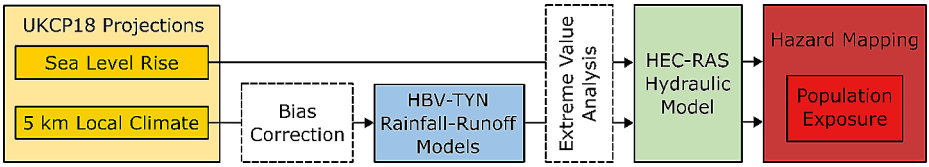

Fig. 1 Methodological framework utilised within this study. After Pasquier (2020)

ies (Fig. 2) were delineated using the 30×30 m resolution Shuttle Radar Topography Mission digital elevation model (Pasquier et al. 2018).

The Broads National Park is the UK's most expansive designated wetland (303 km^2 and 2.7 km of coastline), a network of man-made surface lakes and waterways that hold 28 Sites of Specific Scientific Interest (SSSIs) and a quarter of the UK's rarest flora and fauna species (Broads Authority 2015; Pasquier et al. 2020). These features, in addition to approximate 280 km of navigable waterways within the Broads, generate around £568 million via tourism (Environment Agency 2009; Pasquier et al. 2020). The major underlying bedrock geology of this catchment are chalk and limestone with overlying deposits of glacial alluvium (Environment Agency 2009). This composition aids mitigation of peak flood flows through groundwater infiltration in regions of exposed bedrock, while areas coated by alluvium see enhanced surface runoff and sensitivity to rainfall. As a result of the tidal dominance of the Broads system, saline intrusion is a prominent risk to freshwater aquatic species, causing food shortages and potential large-scale mortality (Environment Agency 2022). With sea level rise promoting propagation of saline waters further upstream, in addition to waning summer river flows, saline intrusion will become a more significant risk and the ability of the hydrological system to flush intruding waters will weaken. Furthermore, the effects of

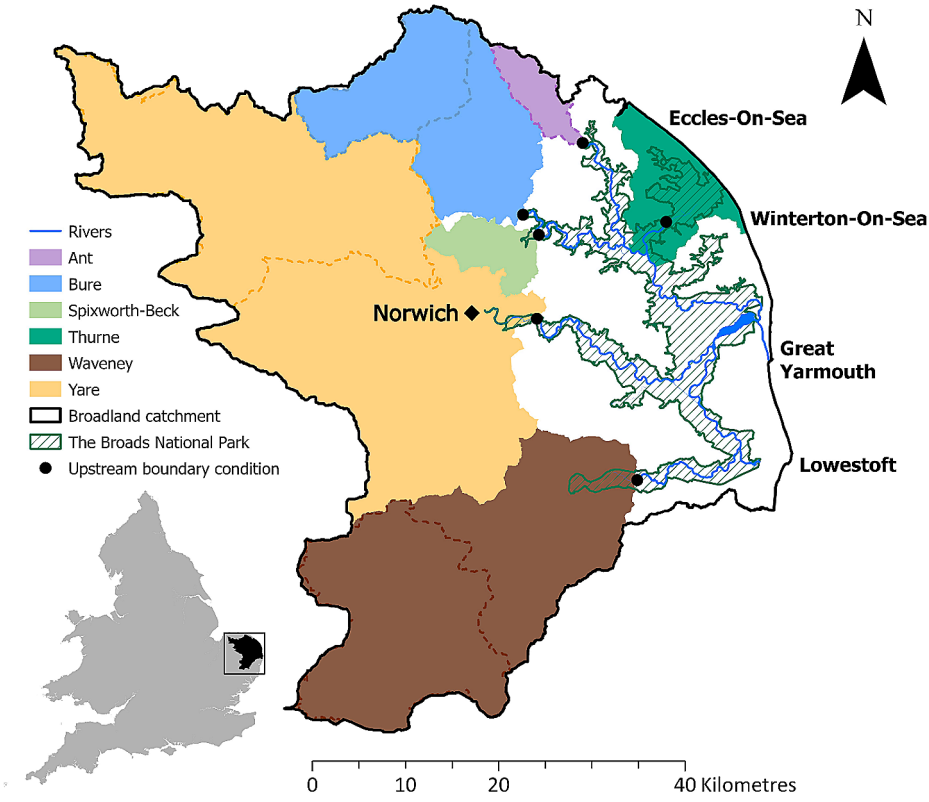

Fig. 2 The Broadland catchment, hydrological sub-catchments, the Broads National Park, and the upstream boundary conditions used within the hydraulic modelling process. Areas within dashed lines represent the four UK National River Flow Archive (NRFA) gauged catchments used for hydrological modelling

sea level rise hold a direct impact on flood risk, with the low-lying nature of the region permitting significant susceptibility to these climate change driven elevations (Pasquier et al. 2020).

2.2 Scenarios

This study produced nine extreme scenarios that simulate a 100-year river discharge event, a 100-year storm surge event and their product, a 10,000-year compound flood for the midpoint of three 20-year time periods (hereafter referred to by their midpoint year): 1990 (reference period), 2030 (mid-term period) and 2070 (long-term period) (Table A1). The UKCP18 RCP8.5 local projections at 5×5 km resolution were used as the climate forcing. The climate model runs at convection-permitting scale for the UK for three time slices (1981–2000, 2021–2040, 2061–2080) produced by the Met Office within the UKCP18 programme (Met Office Hadley Centre 2019).

2.3 Flood modelling

2.3.1 UKCP18 data and bias correction

The UK Climate Projections (UKCP18) is a climate data set produced by the UK Meteorological Office and contains a spectrum of probabilistic projections from the 60 km resolution General Circulation Model (GCM), 12 km Regional Climate Model (RCM) and 2.2 km Convection-permitting Model (CPM) (Met Office 2019; Kendon et al. 2019). The former two can model physical climate feedbacks, climate means and variability at a daily timestep and at national or larger scales (McSweeney and Hausfather 2018; Met Office 2019). The new 2.2 km CPM is more capable of representing physical processes visible at finer resolutions, including atmospheric convection, which can lead to intense storm events, and the influence of mountains, coastlines and urban areas (Met Office 2019). The 5 km CPM projections utilised in this study were regridded from the 2.2 km dataset on the Ordnance Survey's British National Grid (OSGB) and inherit its convection-permitting capacity (Met Office 2018). The 5 km CPM dataset contains 12 ensemble members, each with member has 3 time slices: 1980–2000, 2020–2040 and 2060–2080. The data version used in this study is v20210615.

Systematic errors within climate models can produce inherent biases relative to observations, with downscaled models such as RCMs and CPMs inheriting significant error from large-scale GCMs, alongside additions from further parameterisation of physical processes (Dosio et al. 2012; Cannon et al. 2015). The typical biases include: (1) too frequent low-intensity wet days or ineffective estimation of extreme temperatures due to insufficiency in model parametrisations (Ines and Hansen 2006; Nyunt et al. 2013); and (2) poorly estimated seasonal variation from ineffective representation of the changing precipitation-driving mechanisms throughout the year (Teutschbein and Seibert 2012; Argüeso et al. 2013). Bias correction is an important prerequisite to hydrological modelling that can produce more reliable outputs (Piani et al. 2010; Teutschbein and Seibert 2012; Grillakis et al. 2017). Popular bias correction methods range from linear and nonlinear scaling, where climatic outputs are adjusted by their means, to distribution mapping, which assumes values conform to a particular statistical distribution (Luo et al. 2018). Within this study, a nonparametric

quantile mapping (QM) method was performed in R v 3.6.2 (R Core Team 2023) using the functionality of package *qmap* (Gudmundsson 2016), with no priori statistical distribution assumed, employing an empirical cumulative distribution to estimate empirical percentiles (Adera and Alfredson 2019). The observations used to inform this distribution was that of the 1×1 km resolution HadUK-Grid meteorological dataset (Met Office et al. 2020). This method is appropriate due to its correction of the cumulative distribution function to that of the observational data, instead of solely adjusting means and variance, therefore, benefitting the robustness of the upper quantiles of the modelled output (Gudmundsson et al. 2012; Wang and Chen 2013).

2.3.2 Hydrological modelling

The study employed the Hydrologiska Byråns Vattenbalansavdelning (HBV) model (Bergström 1992; Lindström et al. 1997) which is a conceptual rainfall runoff model utilised for modelling of historical and future fluvial floods (Steele-Dunne et al. 2008; Yin et al. 2021). With deployment for climate impact assessment in academic and functional capacities (Lidén and Harlin 2000; Swedish Meteorological and Hydrological Institute 2014), computational efficiency and robustness amongst a spectrum of climatological and physiographic settings have been thoroughly established (Zhang and Lindström 1996; te Linde et al. 2008; Driessen et al. 2010; Cloke et al. 2012; Kalantari et al. 2012; Beck et al. 2016). Many different HBV model versions exist. The model used in this study is the distributed HBV-TYN similar to He et al. (2022) which was developed from the HBV-IWS model (He et al. 2011). In this study, the model uses 1×1 km precipitation, temperature and potential evapotranspiration as input data. It was calibrated using the daily observed discharge dataset from the UK National River Flow Archive (NRFA), an online repository of monitored flow data from over 1600 UK river gauging stations (NRFA 2023a).

The HBV-TYN model was then driven by the bias corrected 5 km UKCP18 climate projection outputs of daily precipitation, temperature and derived evapotranspiration. They were then downscaled to 1×1 km resolution using bilinear interpolation and used to drive the HBV-TYN model in four catchments (Fig. A3): River Bure (34,003), Wensum (34,004), Waveney (34,006) and Ant (34,008). The numbers in the brackets are the NRFA station numbers. Due to the small extents and minimal topographical inclines of the ungauged catchment segments (as well as the Spixworth-Beck and Thurne), a proxy discharge scaling method was used based on the ratio between the catchment drainage area up to the upper boundary point and the NRFA gauged area (see the scale factors in Table 1). The catchments Ant, Bure, Waveney and Yare use direct conversions from their own gauged catchments,

Table 1 Final scaled base flows and peak flows for all hydraulically modelled catchments in m^3s^{-1}

Upper boundary (UB)	Scaling factor	Base flow			Peak flow		
		1990	2030	2070	1990	2030	2070
Ant (UB01)	1.00	0.29	0.30	0.26	2.31	3.34	3.15
Bure (UB02)	1.99	1.73	1.78	1.46	11.76	15.82	14.42
Spixworth-Beck (UB03)	0.36	0.31	0.32	0.26	2.13	2.86	2.61
Yare (UB04)	2.44	8.40	8.40	6.90	68.34	91.25	91.50
Waveney (UB05)	1.85	2.47	2.32	1.66	99.57	144.84	136.01
Thurne (UB06)	0.21	0.72	0.72	0.59	5.88	7.85	7.87

while the Spixworth-Beck and Thurne are scaled from the Bure and Yare gauged catchments, respectively.

2.3.3 Storm surge

Storm surges represent one of the most significant drivers of flood hazard events when coinciding with peak sea level (Pasquier 2020). The peak surge value from Pasquier (2020) was used where the Revised Joint Probability Method (Environment Agency 2011) was employed that ascribes an 'indirect' method assessing the coinciding likelihood of peak astronomical tide and storm surge. The 3.27 maOD return level was determined in Pasquier (2020) using the reference year 2018. It was then extrapolated to the three time periods (1990, 2030 and 2070) via the UKCP18 sea level rise projections, finding relative differences of -0.05, +0.09 and +0.55 m, respectively (Fig. A1; Table 2). These values were applied to a normalised Lowestoft surge profile (Fig. A2) produced by the Environment Agency (2011) to inform the downstream boundary conditions of the hydraulic model.

2.3.4 Hydraulic modelling

The Hydrologic Engineering Centre's River Analysis System (HEC-RAS) program was selected to simulate catchment hydrodynamics. The software was developed by the U.S. Army Corps of Engineers (Ongdas et al. 2020) and is publicly available. As a fully spatially distributed application, HEC-RAS offers simulation capabilities of channelised 1D steady or unsteady flow, alongside 2D unsteady overland flow (David and Schmalz 2021; Zeiger and Hubbart 2021). HEC-RAS has achieved popularity as a staple standalone modelling tool (Quirogaa et al. 2016; Dasallas et al. 2019), presenting compatibility with GIS, permitting the modelling of diverse hydrological systems and complex flow regimes (Vozinaki et al. 2016; Pasquier 2020). The model employed within this investigation is that of Pasquier (2020), defined by a 2-metre resolution Environment Agency LiDAR digital terrain model with corrected channel bathymetry (Broads Authority 2011–2015 river surveys). Model calibration (featuring Manning's n roughness coefficient as a calibration parameter) and validation utilised Environment Agency historical river levels at 15-minute increments, running initially as steady then unsteady conditions (see Supplementary Information Appendix B for more detailed model setup, calibration and validation descriptions). Required inputs included event boundary conditions of 100-year river discharge flow hydrograph and storm surge stage hydrograph (upper and lower boundary conditions, respectively) (Fig. A4).

2.4 Exposure

Flood rasters (2 m resolution) were extracted from the HEC-RAS model outputs and utilised to derive 'binary exposure' (the intersection of an element with inundation above a critical threshold constituting exposure; Sayers et al. 2020) in human elements, and overlayed onto the 10 m resolution dasymetrically-mapped OpenPopGrid population distribution created

Table 2 Storm surge elevation in m above Ordnance Datum (maOD) for all scenarios

Scenario	Surge height (maOD)
1990	3.22
2030	3.36
2070	3.82

within Murdock et al. (2015). The Humanitarian Data Exchange (HDX) high resolution population density maps discussed in Orusa et al. (2023) were considered, however, OpenPopGrid was selected based on its greater resolution, thus providing better compatibility with HEC-RAS flood maps. Values of risk and exposure were divided into quartiles to represent the magnitude of risk from moderate to very high.

3 Results

3.1 Bias correction

On a monthly basis, raw CPM outputs heavily overestimate precipitation throughout the entire year except in June-October (Fig. 3a). The bias corrected data showed significant improvement in matching with the observational data, with a change of Pearson correlation coefficient R^2 value from 0.207 (raw CPM) to 0.978 (bias corrected CPM), with all changes being consistent across all catchments. The effect of bias correction throughout all periods was evident, with overestimation of winter precipitation corrected for while summer rates remaining more consistent from the raw to bias corrected CPM projections (Fig. 3a-c). Within the annual totals the effect of the bias correction is clear with the processed data mirroring the raw data but at a magnitude closer to that of the HadUK-Grid observed totals (Fig. A5a). The bias corrected range of the annual 5-day maximums (Fig. A5b), also showed greater coherency with the observed.

Despite the better representation of trends in observational data by the raw CPM temperature outputs (R^2 of 0.993 in catchment 34,003), the bias correction again provided a much greater fit (R^2 of 0.9997, 4 s.f.) (Fig. 3d). The climatic trend demonstrated an expected increase in temperature throughout the monthly distribution (Fig. 3d-f). It was also noted that the profile of the monthly variation remained constant, with a consistent underestimation in the raw CPM values. Both the raw and corrected CPM data capture the general increase of temperature shown in observations (Fig. A5c). Furthermore, correction on an annual timescale showed a similar effect to that of precipitation.

3.2 Hydrological modelling

The bias corrected outputs were used to feed into the HBV-TYN model to simulate discharges. Apart from 34,003, all simulated catchments showed reasonable output in terms of magnitude and monthly variation, with baseline means closely fitting to observed NRFA observed gauged discharges. Catchment 34,003 showed an appropriate monthly profile (Fig. 4a); however, it appeared to lag relative to the gauged profile. Furthermore, 34,004, 34,006 and to some degree 34,003 (Fig. 4b, c and a) exhibited greater disparity from the gauged discharges within the period of December to February, with the former two underestimating flow. Evaluation of similarity between the CPM driven outputs and the observational data was performed using the mean absolute percentage error (MAPE) method exhibited in Hannaford et al. (2022). Predominantly, the MAPEs remained below the range detailed for East Anglia catchments in the above study (20–50%). Catchment 34,003 held a MAPE of 13% which is surprising relative to its poor fit with the gauged discharge profile and mediocre Nash–Sutcliffe model efficiency coefficient (NSE) of 0.506. Catchments

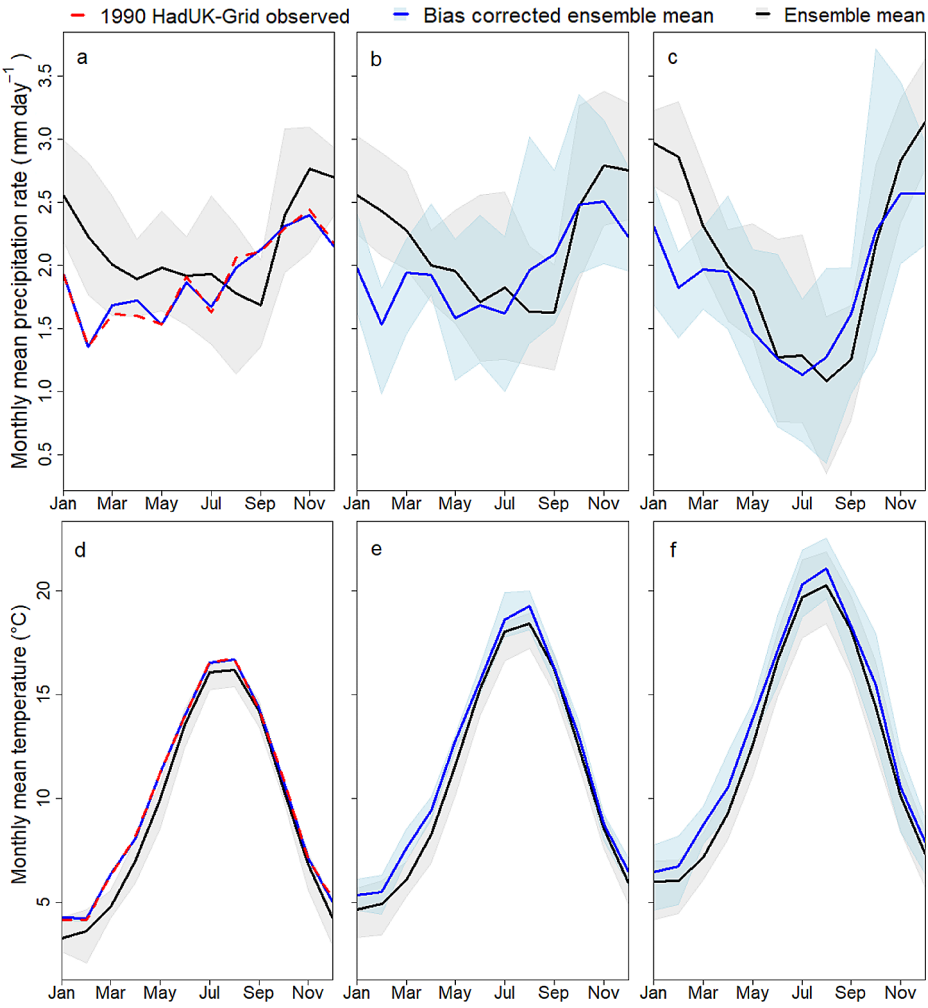

Fig. 3 Monthly mean precipitation rate (mm.day^{-1}) of the baseline HadUK-Grid observations (red), and the raw (black) and bias corrected (blue) CPM data for 1990 **(a)**, 2030 **(b)** and 2070 **(c)** in catchment 34,003 (Bure). Monthly mean temperature (°C) of the baseline HadUK-Grid observations (red), and the raw (black) and bias corrected (blue) CPM data for 1990 **(d)**, 2030 **(e)** and 2070 **(f)** in catchment 34,003 (Bure). The grey and blue shaded areas represent the ranges of the 12 ensemble members from the raw and bias corrected data, respectively

34,004 and 34,006 displayed good scores, at 14 and 27%, respectively, which corroborated with their high NSE values of 0.752 and 0.796. As expected by its fit to the gauged profile, catchment 34,008 (Fig. 4d) displayed the best MAPE of 9.4%; however, this does not corroborate with its poor NSE of -0.368. Despite fluctuation in these statistics, when assessed with the peak error method, all catchments displayed exemplary figures of -0.9, -0.7, -0.7 and −0.6% (Catchments 34,003, 34,004, 34,006 and 34,008, respectively), constituting good model effectiveness at simulating peak values (Rabuffetti et al. 2008).

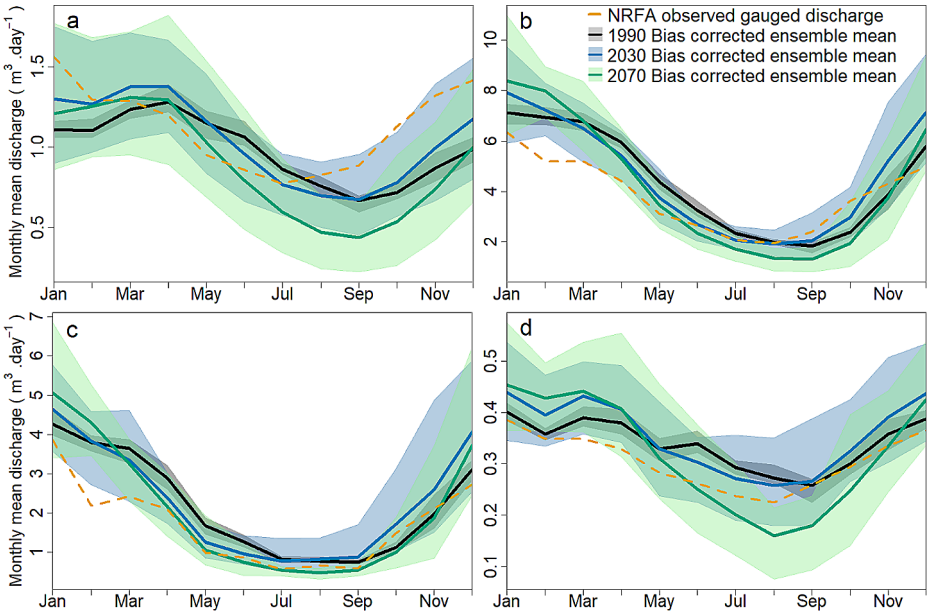

Fig. 4 Monthly mean discharge ($m^3 day^{-1}$) of the NRFA gauged observations (orange) and the simulated discharge in 1990 (black), 2030 (blue) and 2070 (green), for catchments **(a)** 34,003 (Bure), **(b)** 34,004 (Yare), **(c)** 34,006 (Waveney) and **(d)** 34,008 (Ant)

Table 3 Simulated base flow (5th percentile of all simulated discharges) and 100-year return discharge (95th percentile of 100-year return discharges) for all hydrologically modelled catchments over all periods in $m^3 s^{-1}$

Catchment	Base flow			100-year return discharge		
	1990	2030	2070	1990	2030	2070
Bure (34,003)	0.87	0.90	0.73	5.91	7.95	7.25
Wensum (34,004)	3.44	3.44	2.83	28.01	37.40	37.50
Waveney (34,006)	1.34	1.25	0.90	53.82	78.29	73.52
Ant (34,008)	0.29	0.30	0.26	2.31	3.34	3.15

The general temporal trend showed slightly drier summers from 1990 to 2030, which was enhanced in 2070 where monthly summer flows decrease even further (Fig. 4). Additionally, from period to period a partial increase in discharge can be seen in the winter months, enhancing the seasonality of yearly flows.

The 100-year return discharge was obtained by using the Gumbel distribution and the maximum likelihood estimation method. Based on the ensemble of twelve 100-year return discharges driven by the 12 CPM outputs, the 95th percentile was calculated as the 100-year return discharge. The 5th percentile of all the simulated flows was obtained as the base flow. Tables 1 and 3 list the base and peak flows of the 4 modelled catchments and the 6 upper boundary (UB) points, respectively. In Table 1, the upper boundary points are numbered from 1 to 6 clockwise from the northernmost point (see Fig. 2). Base flows showed relative consistency from 1990 to 2030, showing miniscule variation (Tables 1 and 3). The 100-year return discharges show greater variation where significant increase is shown from 1990 to 2030, up to 24.5 $m^3 day^{-1}$ in the Waveney catchment (34,006). The 100-year return

Table 4 Total flooded area (km^2) and population exposed during each flood scenario. See Table A1 for scenarios

Metric	100-year river discharge			100-year storm surge			10,000-year compound		
	1990	2030	2070	1990	2030	2070	1990	2030	2070
Flooded area (km^2)	38.7	53.1	53.3	186	191	204	197	200	208
Population exposed	59	118	161	13,771	13,845	18,633	13,917	14,088	18,785

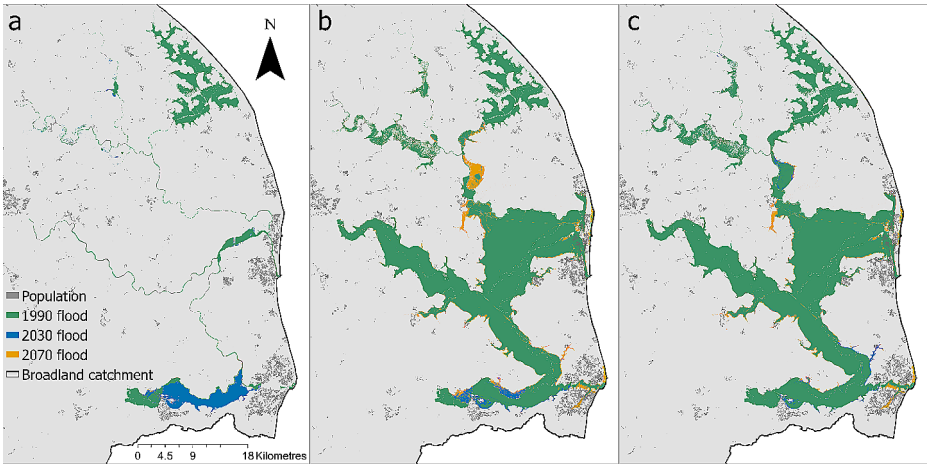

Fig. 5 Extent of all **(a)** 100-year river discharge flood scenarios; **(b)** 100-year storm surge flood scenarios; **(c)** 10,000-year compound flood scenarios

discharges for 2030 and 2070 only show slight positive and negative variations throughout the catchments.

3.3 Hydraulic modelling

In the 1990 time period, the 100-year river discharge event is largely constricted to the main channels of the Broads (Fig. 5a), with a total extent of 38.7 km^2 (Table 4). Exceptions to this are observed in expansive but shallow inundation in the upper reach of the River Thurne, the upper Waveney and intermittent low-lying land along the River Bure. Overall, 1990's flood depths are mainly restricted to a 0–1 m range (Fig. 6a). 2030 sees significant expansion in the core of the Waveney (total of 53.1 km^2; Table 4), with this being matched by the 2070 scenario (53.3 km^2; Table 4). 2030 and 2070 show great likeness, with only minor disparities in extent and flood depth density distribution (Figs. 5a and 6a).

The 1990 100-year storm surge exhibits expansive inundation throughout all riverine limbs of the Broads, with primary flooding throughout its core, the Yare and the Waveney (Fig. 5b), inundating a total extent of 186 km^2 (Table 4). These regions see flood depths within the range of 1–1.5 m (Fig. 6b). Changes from 1990 to 2030 (flooding 191 km^2; Table 4) are primarily shown in the Waveney limb, which thickens due to the heightened surge (Fig. 5b). Furthermore, the density distribution of flood depths spreads out due to increasing areas of greater depths (Fig. 6b). 2070 exhibits further expansion where extru-

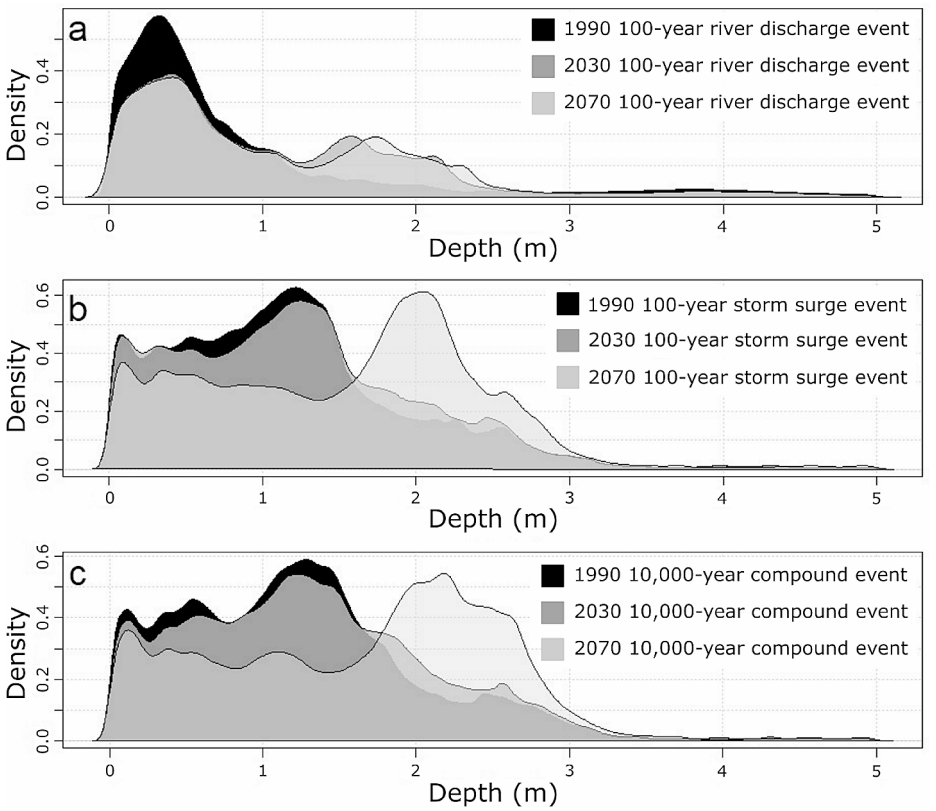

Fig. 6 Kernel density plot of flood depths (m) for all **(a)** 100-year river discharge flood scenarios; **(b)** 100-year storm surge flood scenarios; and **(c)** 10,000-year compound flood scenarios at a 10 m resolution

sions into the land surrounding the Broads, most notably below Lowestoft and in the lower Bure above the large region of marshland, hereafter referred to as the 'core Broadland', which extends out behind Great Yarmouth to where the Rivers' Bure, Waveney and Yare split off, reaching an inundated area of 204 km^2 (Table 4). This results in the flood depth distribution peak shifting into the 1.5–2.5 m range (Fig. 6b).

Documenting total inundated areas of 197, 200 and 208 km^2 (Table 4), the compound events show an additional effect of the co-occurring river discharge and storm surge events. Inundation follows a distribution similar to the 2070 surge scenario, albeit 2070 exhibits a breach into the surrounding land on the west perimeter of the lower Bure that was observed in the 2070 surge as well as more extensive flooding in Lowestoft and Great Yarmouth (Fig. 5c). Similarity to the 100-year storm surge events is shown in Fig. 6c, where 1990 and 2030 share a close likeness with peaks in the 1–1.5 m range and 2070 with a peak in the 1.5–3 m range.

Population exposure follows the same trends as flooded area, with the 100-year river discharge event causing exposures of 59, 118 and 161, for 1990, 2030 and 2070 respectively (Table 4). The same trends are exhibited for the 100-year storm surge and 10,000-year flood events, with magnitudes of 13,771, 13,845 and 18,633 (1990, 2030 and 2070 for the 100-

year storm surge scenario, respectively), and 13,917, 14,088 and 18,785 (1990, 2030 and 2070 for the 10,000-year compound scenario, respectively).

4 Discussion

4.1 Bias correction and HBV performance

Bias correction is a key post-processing technique to account for systematic bias induced by sources such as poor representation of climate forcing responses, unpredictable internal variability within the baseline period, or faults in model parametrisation (Cannon et al. 2015). The non-parametric Quantile mapping bias correction applied within this study proved effective, where bias in the form of overestimation of winter highs in precipitation from the UKCP18 5 km convection permitting model saw appropriate adjustment relative to the HadUK-Grid observational data within the baseline (1980–2000) period (Fig. 3a). Similar effects were observed in the 12 km RCM predecessor (Pasquier 2020) and were considered to result from biases in the original GCM (Dosio et al. 2012). This effectiveness of bias correction was also evident for temperature, where slight underestimations were observed prior to correction. Nevertheless, the hydrology in the Broadland catchment is primarily driven by precipitation changes so temperature effects are minimal (Pasquier 2020). A specific limitation of Quantile mapping is seen in its difficulty in retaining climate signals via application of the determined statistical distribution of the calibration period to future scenarios. However, nonparametric transformation mitigates this effect by not assuming a theoretical distribution (Hempel et al. 2013; Wang and Chen 2013; Gudmundsson et al. 2012). Evidently, the bias correction process can preserve the climate signal while providing observation-based corrections and may simultaneously correct for overestimation of precipitation amounts in the raw CPM forecasts. Most importantly, however, the climatic changes predicted by each CPM ensemble member are retained throughout the correction process. This was most evident in the 2060–2080 period where the bias corrected CPM data captured the deepening of the summer lows and enhancement of winter highs within the precipitation monthly variation (Fig. 3c). Preservation of the long-term trend was also displayed in the temperature bias correction (Fig. 3d-f), where the warming effect was retained while appropriate reductions were made to reduce model bias observed in the calibration period. These effects are successfully modelled by the HBV-TYN model, showing the model's efficacy in predicting future flows, although, evaluation may be complicated by factors affecting runoff within sub-catchments (Pasquier 2020; NRFA 2023b).

4.2 Flood simulations

Coastal flooding represents one of the most significant and common threats in both a global and UK-specific context (He et al. 2013; Haigh et al. 2016), with the Broadland catchment exhibiting one such extensive history of flooding (Norfolk County Council 2015). Flooding within the Broadland catchment has been priorly simulated in the contexts of extreme river discharge and tidal surges, alongside associated climatic changes. One such study, Pasquier et al. (2018) explored inundation within the Broads region from Great Yarmouth northwards. Pasquier et al. (2018) scenario 2mQ100 (a 2-metre mean SLR 100-year storm surge

event in parallel with a 100-year river discharge event) showed greater flooding through the Filby Broad than the 2070 compound scenario (Fig. 5c), although, 2mQ100 scenario is based in 2100 with 2 m sea level rise, while the sea level rise exhibited to the 2070 in this study only documents an elevation of 0.55 m from 1990 (Table 2). Nevertheless, this elevation produces significant propagation and expansion of inundation along the Waveney limb of the Broads in each surge-related scenario, as well as its bordering tributaries, due to its shallow elevation profile and proximity to the surge-dominant core Broadland (Figs. 2 and 5b). Despite this, it is worth noting that the 100-year river discharge event exhibits significant fluvial influence in the Waveney limb (Fig. 5a), suggesting a more complex hydrological regime in this region. 1mQ100 (2mQ100 reduced to only 1-metre mean SLR) displayed more similar flood patterns to the 2070 event with lesser depths in the central Broads where the 2070 scenario exhibited greater homogeneity in flood depths within the 1–2 m range. Despite these greater depths, the 2070 event does not detail the same expanse of flooding around the junctions of the Ant, Bure and Thurne, where 1mQ100 shows a large extent of 1–3 m flooding. In this instance, the 2070 flooding in the Bure sub-catchment is closer to the 2100Q0 or 1mQ0 scenarios (both do not simulate the occurrence of the 100-year river discharge event). This similarity in the absence of the river discharge component further highlights the tidal dominance of the Broads system, where the storm surge component exhibits a much more significant extent of inundation. One disparity, however, is observed in scenario 2100Q100 (a 100-year storm surge at a mean SLR of 4 $mm.a^{-1}$ coinciding with a 100-year river discharge event) which experiences significantly greater flooding in along the reach of the Bure prior to joining the core Broadland area (Pasquier et al. 2018). This is despite a lower 100-year peak river discharge at the 99th percentile of 6.83 $m^3.s^{-1}$ for the Bure (compared to this study with 11.76, 15.82, 14.42 $m^3.s^{-1}$, for 1990, 2030 and 2070, respectively), which may again point to the dominance of the surge component in inundation events. These differences between scenarios illustrate the requirement for simulation of an ensemble of futures and hazard compositions to establish the range of flood hazard impact.

The core comparison is between the presented scenarios and RCP8.5 scenarios modelled in Pasquier (2020). Pasquier (2020) shows similar distribution of flooding within a 100-year river discharge event, although this study displays more extensive spread of shallow inundation in the floodplain between the upper Thurne and the coast. Disparities between the various scenarios are explored to a greater extent within this study, with inclusion of both the independent 100-year component events and their compound throughout all three time periods. This provides insight into the magnitude of flooding attributed to each component flood factor, where the tidal influence described in CH2M (2016) is illustrated by the dominance of the storm surge for defining the distribution of the compound events. Although sea level rise is the primary driving force, producing dominance of storm surge in determining future flood dynamics and variation, the simulation of the 100-year river discharge events provides insight into the future influence of meteorological changes. The upstream boundary conditions defined by these meteorological changes exhibit a shared trend of significant promotion of 100-year river discharge from 1990 to 2030 (Table 1) in parallel to major flood expansion in the Broadland limb that intersects the Waveney catchment (Fig. 5a), before remaining relatively consistent to 2070. This is corroborated by the kernel density distribution of flood depths within the 100-year river discharge scenario, where the distribution flattens, with peaks emerging at the greater range of 1.5–2.5 m (Fig. 6a).

Pasquier (2020) also presents RCP8.5 10,000-year compound floods scenarios, to which the 2030 events are directly comparable, where somewhat similar flood distributions were shown with the core Broad and limbs of the River Yare and Waveney featuring most of the inundation. However, the event simulated in this study documents a greater coverage of 1–2 m depths throughout these regions, as well as greater propagation of shallow floodwaters northwards, while Pasquier (2020) exhibits a greater proportion of 2–3 m flooding in the Yare and Waveney sub-catchments. Similarity is expected due to 100-year river discharges residing within the ranges described by Pasquier (2020) for the 2020–2080 period. However, it is observed that the Rivers Ant, Bure, Spixworth Beck and Thurne hold 100-year flows (Table 1) below the stated 100-year means of the extended period of Pasquier (2020), potentially explaining the lower maximum depths of flooding in the modelled 2030 flood. Again, the 2070 flood has coherence with the 2055 and 2080 scenarios, which includes the extension of flooding southwards from Lowestoft and northwards into the junction of the River Thurne. Disparities were shown, with greater 3–4 m inundation in the 2055 and 2080 simulations within the Yare sub-catchment (Pasquier 2020). Furthermore, a greater extent of 1–2 m floodwater in the 2030 scenario propagated beyond the north-eastern edge of the core Broadland, between the villages of Stokesby and Tunstall, which represents a consistent boundary for the extent of major flooding in all simulations presented in Pasquier (2020). Furthermore, flooding in the Broads via tidal surge from Eccles-On-Sea to Winterton-On-Sea is relatively limited in Pasquier (2020). It is worth noting that all scenarios within the presented study occupy a midground between Pasquier (2020) and the CH2M (2016) present day 200-year tidal flood. Throughout these, the echoed outcome is that extreme flood events will face enhancement into the future, holding more severe consequences. While this is illustrated by the 10,000-year compound flood event that is an extreme worst-case scenario, its' simulation carries significant potential for establishing the sensitivity of the Broadland catchments to multiple flood mechanisms.

4.3 Exposure

Population exposure has no such empirical damage function, so critical thresholds must be utilised, with this study setting this limit at the simple presence of inundation (Sayers et al. 2020). Comparisons can only be directly drawn from Environment Agency (2009) which establishes 3,900 people at risk from flooding from 100-year river discharge and 200-year tidal flood. However, these flood extents are applied independently rather than compounding. Therefore, the amalgamative nature of the events simulated here remain plausible, corroborating with the Environment Agency's predictions of increases to 14,360 people at risk in Great Yarmouth and Lowestoft by 2100. Exponential increases in both property and population exposure are widely corroborated, with key assessment seen with the Third UK Climate Change Risk Assessment (CCRA3) Future Flood Risk report where six-fold and ten-fold increases in exposed UK residential properties are projected in 2 and 4 °C futures (2100), respectively, while swells in population exposure by a third to nearly three-fold are seen in low and high population growth futures (Sayers et al. 2020, 2022).

4.4 Assumptions and limitations

The study saw a primary limitation from the ungauged Spixworth-Beck and Thurne sub-catchments, prompting the assumption that these hydrological systems were similar enough to others for a proxy method to be applied. The storm surge return value was obtained from Pasquier (2020). Future studies could update the value with new observational data. Further limitation within the modelling process was the lack of inundation extent data for the HEC-RAS model validation, however, the use of tide gauge river level data was deemed an appropriate proxy for this tidal flooding scenario. Population exposure was limited by a lack of dasymetric population distribution informed by the 2021 UK Census, restricting the reference year to 2015. Finally, a core assumption is the stationarity of distributions of population during different time periods, where research could benefit from observing interactions of flood and population changes as exposure might be underestimated as a result.

Another major factor of influence is uncertainty. The major source of uncertainty originates from the UKCP18 projections and was considered by using the ensemble mean of the 12 members of the UKCP18 projection. The data uncertainty was minimised when possible, by utilising the highest resolution data available (e.g. 2-metre resolution LiDAR data and 1-kilometre resolution meteorological data), but uncertainties can be inherited through the various processing steps. They include the resampling of the 2.2 km UKCP18 CPM projections to 5 km resolution, downscaling of the 5 km to 1 km resolution, and bias correction of the projected precipitation and temperature. Uncertainties can also come from the hydrological and hydraulic models cascade chain used in this study (Cloke et al. 2012; He et al. 2009). Future studies can improve upon the current study by considering the total uncertainties starting from climatic projections through data processing and to the impact models cascade chain.

5 Conclusions

Development and integration of all sequential components within the modelling chain has produced a robust and high-resolution hazard modelling framework that could be utilised to inform catchment level flood risk management policy. State-of-the-art data and techniques have been included to produce a forward-thinking and adaptive assessment tool, with successful utilisation of a climate-responsive nonparametric bias correction and the distributed HBV-TYN model. Key results document an increasing severity of flooding within a high emission future, with exponential impacts over time where flood magnitude shows greater increase from 2030 to 2070 (increase of 8 km^2 inundated area and 4,697 people exposed in the compound events) than from 1990 to 2030 (increase of 3 km^2 inundated area and 171 people exposed in the compound events). Results exhibit a lesser effect of isolated 100-year river discharge events (maximum in 2070 with 53.3 km^2 flooded and 161 people exposed) compared to that of a 100-year storm surge event (maximum in 2070 of 204 km^2 flooded and 18,633 people exposed), showing the dominant effect of sea level rise relative to meteorological variation. Furthermore, a 10,000-year compound scenario where the two are modelled simultaneously projects an amalgamated effect (maximum in 2070 of 208 km^2 flooded and 18,785 people exposed), although, the storm surge component remains significantly dominant. Despite this dominance, meteorological influence is observed in the river

discharge scenario, with significant temporal variation (1990 to 2030) in the River Waveney. While a large proportion of floodwater is contained within the core Broadlands' floodplains, mass riverbank overtopping occurs along the main Broadlands' river limbs.

These simulations represent an extreme scenario that traditional flood management plans could not feasibly prevent, although a significant proportion of inundation impacts grazing marshland within the Broads rather than urban settlements, showing the retention capabilities of the Broads hydrological system. Nevertheless, future management may benefit from additional measures such as nature–based solutions which provide more adaptive mitigation of inundation (Ruangpan et al. 2020). More recent policy observes the integration of natural flood management, a methodology that aims to increase upstream flood water storage and attenuate the flow hydrograph peak (Environment Agency 2018). This scheme involves techniques such as peatland restoration and reconnecting floodplains, with implementation planned in five locations in Norfolk as funded by Defra who announced the programme in 2017.

Previous research has shown that compound flood risk is a growing concern for coastal areas around the world (Couasnon et al. 2020). While the assessment of flood hazard and impacts requires a careful understanding of site-specific processes, this research can provide broader insights for other regions. A modelling framework to characterize the impacts of compound flooding under climate change was presented, which can be replicated using global datasets (Eilander et al. 2023). An important challenge in assessing the impacts of compound flooding is the representation of different sources of flooding in complex low-lying coastal environments. The integrated HBV-TYN and 1D/2D HEC-RAS approach provides a flexible modelling tool to represent large areas with a high level of detail while limiting computational costs and can therefore be suited to a wide range of locations.

Future research would benefit from expansion of the range of scenarios, primarily following diverse emissions pathways to account for future uncertainties, alongside a suite of return periods to assess effects a range of flood magnitudes. Improvement could involve using higher resolution data, with UKCP18 2.2 km data enabling hourly bias correction to better represent peak rainfall and consequently peak discharges. Additional components could be appended, with analysis of the mitigation capacity of various measures, namely nature-based solutions or National Flood Management. A more comprehensive exposure derivation could be implemented to increase accuracy and see the application of depth-damage functions to disaggregated units. Within the exposure component, non-stationarity could be explored with the consideration of changes in population.

Supplementary Information The online version contains supplementary material available at https://doi.org/10.1007/s11069-024-06590-5.

Author contributions RG and YH contributed to the study's conceptualisation and design. RG and UP contributed to material preparation, data collection and the HEC-RAS model setup. YH performed the HBV-TYN model simulation. RG, NF, CN, QZ, YH and UP contributed to the scripts and analysis. The first draft of the manuscript was written by RG and all authors commented and edited the manuscript.

Funding Author YH has received research support from a NERC funded project: OpenCLIM (Open CLimate Impacts Modelling framework) (NE/T013931/1). Author NF has received research support from the Faculty of Science of the UEA and Amar-Franses and Foster-Jenkins Trust.

Declarations

Competing Interests The authors have no relevant financial or non-financial interests to disclose.

References

Adera AG, Alfredsen KT (2019) Climate change and hydrological analysis of Tekeze river basin Ethiopia: implication for potential hydropower production. J Water Clim Change. https://doi.org/10.2166/wcc.2019.203

Adger WN, Hughes TP, Folke C et al (2005) Social-ecological resilience to coastal disasters. Science 309(5737):1036–1039. https://doi.org/10.1126/science.1112122

Argüeso D, Evans JP, Fita L (2013) Precipitation bias correction of very high resolution regional climate models. Hydrol Earth Syst Sci 17(11):4379–4388. https://doi.org/10.5194/hess-17-4379-2013

Bates PD, Savage J, Wing O, Quinn N, Sampson C, Neal J, Smith A (2023) A climate-conditioned catastrophe risk model for UK flooding. Nat Hazards Earth Syst Sci 23:891–908. https://doi.org/10.5194/nhess-23-891-2023

Baxter PJ (2005) The east coast Big Flood, 31 January–1 February 1953: a summary of the human disaster. Philosophical Trans Royal Soc A: Math Phys Eng Sci 363(1831):1293–1312. https://doi.org/10.1098/rsta.2005.1569

Beck HE, van Dijk AIJM, de Roo A et al (2016) Global-scale regionalization of hydrologic model parameters. Water Resour Res 52(5):3599–3622. https://doi.org/10.1002/2015wr018247

Bergström S (1992) The HBV model: its structure and applications. SMHI, Norrköping

Bradley SL, Milne GA, Teferle FN et al (2009) Glacial isostatic adjustment of the British Isles: new constraints from GPS measurements of crustal motion. Geophys J Int 178:14–22. https://doi.org/10.1111/j.1365-246x.2008.04033.x

Broads Authority (2014) Broadland rivers catchment plan. https://broadlandcatchmentpartnership.org.uk/wp-content/uploads/2018/08/Catchment-Plan-website-final.pdf. Accessed 17 September 2022

Broads Authority (2015) Broads climate change adaptation plan report by head of strategy and projects. https://www.broads-authority.gov.uk/__data/assets/pdf_file/0014/200651/Climate-Change-Adaptation-Plan.pdf. Accessed 19 September 2022

Cabinet Office (2010) National risk register of civil emergencies. https://www.gov.uk/government/publications/national-risk-register-for-civil-emergencies-2010-edition. Accessed 24 February 2024

Cannon AJ, Sobie SR, Murdock TQ (2015) Bias correction of GCM precipitation by quantile mapping: how well do methods preserve changes in quantiles and extremes? J Clim 28(17):6938–6959. https://doi.org/10.1175/jcli-d-14-00754.1

CH2M (2016) A flood management high level review for the Broads climate partnership. https://www.broads-authority.gov.uk/__data/assets/pdf_file/0011/230015/A-Flood-Management-High-Level-Review-for-the-Broads-Climate-Partnership.pdf. Accessed 12 July 2022

Chatterton J, Viavattene C, Morris J et al (2010) The costs of the summer 2007 floods in England. SC070039/R1 Environment Agency, Bristol, Project

Cloke HL, Wetterhall F, He Y (2012) Modelling climate impact on floods with ensemble climate projections. Quarterly Journal of the Royal Meteorological Society, 139(671):282–297. https://doi.org/10.1002/qj.1998

Couasnon A, Eilander D, Muis S et al (2020) Measuring compound flood potential from river discharge and storm surge extremes at the global scale. Natural Hazards Earth System Sciences, 20:489–504. https://doi.org/10.5194/nhess-20-489-2020

Dasallas L, Kim Y, An H (2019) Case study of HEC-RAS 1D–2D coupling simulation: 2002 Baeksan flood event in Korea. Water 11(10):2048. https://doi.org/10.3390/w11102048

David A, Schmalz B (2021) A systematic analysis of the interaction between rain-on-grid-simulations and spatial resolution in 2D hydrodynamic modelling. Water 13(17):2346. https://doi.org/10.3390/w13172346

Day SA, O'Riordan T, Bryson J et al (2015) Many stakeholders, multiple perspectives: long-term planning for a Future Coast. Adv Global Change Res 299–323. https://doi.org/10.1007/978-94-007-5258-0_12

Defra (2006a) Shoreline management plan guidance volume 1: aims and requirements. https://assets.publishing.service.gov.uk/government/uploads/system/uploads/attachment_data/file/69206/pb11726-smpg-vol1-060308.pdf. Accessed 26 December 2023

Defra (2006b) Shoreline management plan guidance volume 2: procedures. https://assets.publishing.service.gov.uk/media/5a75c748ed915d506ee8168d/pb11726v2-smpg-vol2-060523.pdf. Accessed 26 December 2023

Defra, The UK Climate Change Risk Assessment 2012 Government Report (2012): 488. https://assets.publishing.service.gov.uk/media/5a78a060e5274a277e68e336/pb13698-climate-risk-assessment.pdf. Accessed 27 February 2024

Dosio A, Paruolo P, Rojas R (2012) Bias correction of the ensembles high resolution climate change projections for use by impact models: analysis of the climate change signal. J Geophys Research: Atmos 117(D17). https://doi.org/10.1029/2012jd017968

Driessen TLA, Hurkmans RTWL, Terink W The hydrological response of the Ourthe catchment to climate change as modelled by the HBV model. Hydrology and Earth System Sciences, 14(4):651–665., https://doi.org/10.5194/hess-14-651-2010

Eilander D, Couasnon D, Sperna Weiland A et al (2010) FC, (2023) Modeling compound flood risk and risk reduction using a globally applicable framework: a pilot in the Sofala province of Mozambique. Natural Hazards Earth System Sciences, 23:2251–2272. https://doi.org/10.5194/nhess-23-2251-2023

Environment Agency (2009) Broadland rivers catchment flood management plan. https://assets.publishing.service.gov.uk/government/uploads/system/uploads/attachment_data/file/288882/Broadland_Rivers_Catchment_Flood_Management_Plan.pdf. Accessed 20 July 2022

Environment Agency (2022) Saline incursion on the Norfolk Broads - Creating a better place. environmentagency.blog.gov.uk. https://environmentagency.blog.gov.uk/2022/12/02/saline-incursion-on-the-norfolk-broads/. Accessed 1 October 2022

Environment Agency (2012) Kelling to Lowestoft Ness shoreline management plan. https://environment.data.gov.uk/shoreline-planning/documents/SMP6%2FKelling%20to%20Lowestoft%20Ness%20SMP%20-%20final.pdf. Accessed 1 March 2024

Environment Agency (2013) Risk of flooding from surface water. https://assets.publishing.service.gov.uk/media/5a7c1bdee5274a1f5cc75d70/LIT_8986_eff63d.pdf. Accessed 26 December 2023

Environment Agency (2016) The costs and impacts of the winter 2013 to 2014 floods. https://www.gov.uk/flood-and-coastal-erosion-risk-management-research-reports/the-costs-and-impacts-of-the-winter-2013-to-2014-floods. Accessed 24 February 2024

Environment Agency (2018) Working with nature to reduce flood risk in Norfolk. https://www.gov.uk/government/news/working-with-nature-to-reduce-flood-risk-in-norfolk. Accessed 3 December 2022

Environment Agency (2021) Broadland flood alleviation project reaches 20 year landmark. https://www.gov.uk/government/news/broadland-flood-alleviation-project-reaches-20-year-landmark. Accessed 24 June 2022

Environment Agency (2011) Coastal flood boundary conditions for UK mainland and islands. https://assets.publishing.service.gov.uk/media/603653898fa8f5481378420b/Design_sea_levels_technical_report.pdf. Accessed 20 September 2022

Gould IJ, Wright I, Collison M et al (2020) The impact of coastal flooding on agriculture: a case-study of Lincolnshire, United Kingdom. Land Degrad Dev 31(12):1545–1559. https://doi.org/10.1002/ldr.3551

Grillakis MG, Koutroulis AG, Daliakopoulos IN, Tsanis IK (2017) A method to preserve trends in quantile mapping bias correction of climate modelled temperature. Earth Sys Dyn 8(3):889–900. https://doi.org/10.5194/esd-8-889-2017

Gudmundsson L (2016) Package 'qmap'. https://cran.r-project.org/web/packages/qmap/qmap.pdf. Accessed 27 June 2022

Gudmundsson L, Bremnes JB, Haugen JE, Engen-Skaugen T (2012) Technical note: Downscaling RCM precipitation to the station scale using statistical transformations – a comparison of methods. Hydrol Earth Syst Sci 16(9):3383–3390. https://doi.org/10.5194/hess-16-3383-2012

Haigh ID, Wadey MP, Wahl T, et al (2016) Spatial and temporal analysis of extreme sea level and storm surge events around the coastline of the UK. Scientific Data 3(1). https://doi.org/10.1038/sdata.2016.107

Hannaford J, Mackay J, Ascott M et al (2022) eFLaG: enhanced future FLows and Groundwater. A national dataset of hydrological projections based on UKCP18. https://doi.org/10.5194/essd-2022-40. Earth System Science Data Discussions

He Y, Wetterhall F, Cloke HL et al (2009) Tracking the uncertainty in flood alerts driven by grand ensemble weather predictions. Meteorol Appl 16(1):91–101. https://doi.org/10.1002/met.132
He Y, Bárdossy A, Zehe E (2011) A catchment classification scheme using local variance reduction method. J Hydrol 411(1–2):140–154. https://doi.org/10.1016/j.jhydrol.2011.09.042
He Y, Pappenberger F, Manful D et al (2013) Flood inundation dynamics and socioeconomic vulnerability under environmental change. Flood Risk Manage Europe 241–255. https://doi.org/10.1016/b978-0-12-384703-4.00508-6
He Y, Manful D, Warren R et al (2022) Quantification of impacts between 1.5 and 4°C of global warming on flooding risks in six countries. Clim Change 170(1–2). https://doi.org/10.1007/s10584-021-03289-5
Hempel S, Frieler K, Warszawski L et al (2013) A trend-preserving bias correction – the ISI-MIP approach. Earth Sys Dyn 4(2):219–236. https://doi.org/10.5194/esd-4-219-2013
Hooton S (2015) Climate change adaptation plan. https://www.broads-authority.gov.uk/__data/assets/pdf_file/0014/200651/Climate-Change-Adaptation-Plan.pdf. Accessed 2 September 2022
Horsburgh KJ, Williams JA, Flowerdew J, Mylne K (2008) Aspects of operational forecast model skill during an extreme storm surge event. J Flood Risk Manag 1:213–221. https://doi.org/10.1111/j.1753-318x.2008.00020.x
Ines AVM, Hansen JW (2006) Bias correction of daily GCM rainfall for crop simulation studies. Agric for Meteorol 138(1–4):44–53. https://doi.org/10.1016/j.agrformet.2006.03.009
Jonkman SN, Vrijling JK, Vrouwenvelder ACWM (2008) Methods for the estimation of loss of life due to floods: a literature review and a proposal for a new method. Nat Hazards 46:353–389. https://doi.org/10.1007/s11069-008-9227-5
Kalantari Z, Jansson PE, Stolte J et al (2012) Usefulness of four hydrological models in simulating high-resolution discharge dynamics of a catchment adjacent to a road. Hydrol Earth Syst Sci Dis. 9:5121–5165. https://doi.org/10.5194/hessd-9-5121-2012
Kendon EJ, Fosser G, Murphy J et al (2019) UKCP18 Convection-permitting model projections: science report, Met Office. https://www.metoffice.gov.uk/pub/data/weather/uk/ukcp18/science-reports/UKCP-Convection-permitting-model-projections-report.pdf
Klerk WJ, Winsemius HC, van Verseveld WJ et al (2015) The co-incidence of storm surges and extreme discharges within the Rhine–Meuse Delta. Environ Res Lett 10(3):035005. https://doi.org/10.1088/1748-9326/10/3/035005
Lidén R, Harlin J (2000) Analysis of conceptual rainfall–runoff modelling performance in different climates. J Hydrol 238(3–4):231–247. https://doi.org/10.1016/s0022-1694(00)00330-9
Lindström G, Johansson B, Persson M et al (1997) Development and test of the distributed HBV-96 hydrological model. J Hydrol 201(1–4):272–288. https://doi.org/10.1016/s0022-1694(97)00041-3
Luo M, Liu T, Meng F et al (2018) Comparing bias correction methods used in downscaling precipitation and temperature from regional climate models: a case study from the Kaidu river basin in Western China. Water 10(8):1046. https://doi.org/10.3390/w10081046
Matless D (2019) Checking the sea: geographies of authority on the East Norfolk Coast (1790–1932). Rural History 30:215–240. https://doi.org/10.1017/s0956793319000207
McSweeney R, Hausfather Z (2018) Q&A: How do climate models work? Carbon brief. https://www.carbonbrief.org/qa-how-do-climate-models-work/. Accessed 30 December 2022
Met Office (2018) UKCP18 guidance: data availability, access and formats. https://www.metoffice.gov.uk/binaries/content/assets/metofficegovuk/pdf/research/ukcp/ukcp18-guidance-data-availability-access-and-formats.pdf. Accessed 14 July 2022
Met Office (2019) UKCP18 factsheet: UKCP local (2.2km) projections. https://www.metoffice.gov.uk/binaries/content/assets/metofficegovuk/pdf/research/ukcp/ukcp18-factsheet-local-2.2km.pdf. Accessed 14 July 2022
Met Office Hadley Centre (2019) UKCP18 convection-permitting model projections for the UK at 2.2km resolution. NERC EDS Centre for Environmental Data Analysis. http://catalogue.ceda.ac.uk/uuid/ad2ac0ddd3f34210b0d6e19bfc335539. Accessed 17 July 2022
Met Office Hadley Centre (2019) UKCP local projections on a 5km grid over the UK for 1980–2080. Centre for Environmental Data Analysis 2023. https://catalogue.ceda.ac.uk/uuid/e304987739e04cdc960598fa5e4439d0. Accessed 4 July 2022
Met Office, Hollis D, McCarthy M et al (2020) HadUK-Grid gridded climate observations on a 1km grid over the UK, v1.0.2.1 (1862–2019). Centre for Environmental Data Analysis, 2020. https://doi.org/10.5285/89908dfcb97b4a28976df806b4818639
Mokrech M, Nicholls RJ, Dawson RJ (2012) Scenarios of future built environment for coastal risk assessment of climate change using a GIS-based multicriteria analysis. Environ Plan 39(1):120–136. https://doi.org/10.1068/b36077
Mosby G (1939) The Horsey Flood, 1938: an example of storm effect on a low coast. Geographical J 93(5):413–413. https://doi.org/10.2307/1788711

Murdock AP, Harfoot AJP, Martin D et al (2015) OpenPopGrid: an open gridded population dataset for England and Wales. GeoData, University of Southampton

Norfolk County Council (2015) Norfolk local flood risk management strategy. https://www.norfolk.gov.uk/39041. 5 August 2022

NRFA (2023a) National River Flow Archive. National River Flow Archive. https://nrfa.ceh.ac.uk/. Accessed 14 April 2023

NRFA (2023b) NRFA station data for 34003 - Bure at Ingworth. National River Flow Archive. https://nrfa.ceh.ac.uk/data/station/info/34003. Accessed 15 April 2023

Nyunt CT, Koike T, Sanchez PAJ et al (2013) Bias correction method for climate change impact assessments in the Philippines. J Japan Soc Civil Eng Ser B1 (Hydraulic Engineering) 69(4):19–24. https://doi.org/10.2208/jscejhe.69.I_19

Ongdas N, Akiyanova F, Karakulov Y et al (2020) Application of HEC-RAS (2D) for flood hazard maps generation for Yesil (Ishim) River in Kazakhstan. Water 12(10):2672. https://doi.org/10.3390/w12102672

Oppenheimer M, Glavovic BC, Hinkel J et al (2019) In: Pörtner HO, Roberts DC, Masson-Delmotte V et al (eds) IPCC Special Report on the ocean and cryosphere in a changing climate. Cambridge University Press, Cambridge, UK and New York, NY, USA, pp 321–445. https://doi.org/10.1017/9781009157964.006

Orusa T, Viani A, Moyo B, Cammareri D, Mondino EB (2023) Risk assessment of rising temperatures using landsat 4–9 LST time series and Meta® Population dataset: an application in Aosta Valley. NW Italy 15(9):2348–2348. https://doi.org/10.3390/rs15092348

Pasquier U, He Y, Hooton S et al (2018) An integrated 1D–2D hydraulic modelling approach to assess the sensitivity of a coastal region to compound flooding hazard under climate change. Nat Hazards 98(3):915–937. https://doi.org/10.1007/s11069-018-3462-1

Pasquier U, Few R, Goulden MC et al (2020) We can't do it on our own!'— integrating stakeholder and scientific knowledge of future flood risk to inform climate change adaptation planning in a coastal region. Environ Sci Policy 103:50–57. https://doi.org/10.1016/j.envsci.2019.10.016

Pasquier U (2020) Modelling future flood risks for inland and coastal adaptation planning. https://ueaeprints.uea.ac.uk/id/eprint/93979/. Accessed 28 December 2023

Pfeffer WT, Harper JT, O'Neel S (2008) Kinematic constraints on glacier contributions to 21st-century sea-level rise. Science 321(5894):1340–1343. https://doi.org/10.1126/science.1159099

Piani C, Weedon GP, Best M et al (2010) Statistical bias correction of global simulated daily precipitation and temperature for the application of hydrological models. J Hydrol 395(3–4):199–215. https://doi.org/10.1016/j.jhydrol.2010.10.024

Quirogaa VM, Kurea S, Udoa K, Manoa A (2016) Application of 2D numerical simulation for the analysis of the February 2014 Bolivian Amazonia flood: application of the new HEC-RAS version 5. Ribagua 3(1):25–33. https://doi.org/10.1016/j.riba.2015.12.001

R Core Team (2023) R: a language and environment for statistical computing. R Foundation for Statistical Computing, Vienna, Austria. https://www.R-project.org/. Accessed 24 November 2023

Rabuffetti D, Ravazzani G, Corbari C, Mancini M (2008) Verification of operational quantitative discharge Forecast (QDF) for a regional warning system – the AMPHORE case studies in the upper Po River. Nat Hazards Earth Syst Sci 8(1):161–173. https://doi.org/10.5194/nhess-8-161-2008

Ruangpan L, Vojinovic Z, Di Sabatino S et al (2020) Nature-based solutions for hydro-meteorological risk reduction: a state-of-the-art review of the research area. Nat Hazards Earth Syst Sci 20(1):243–270. https://doi.org/10.5194/nhess-20-243-2020

Sayers P, Horritt M, Penning-Rowsell E (n.d.) Future Flood Explorer. http://www.sayersandpartners.co.uk/uploads/6/2/0/9/6209349/ffe_flyer.pdf. Accessed 4 October 2022

Sayers P, Horritt M, Carr S et al (2020) Third UK Climate Change Risk Assessment (CCRA3): future flood risk. Research undertaken by Sayers and Partners for the Committee on Climate Change. Committee on Climate Change, London

Sayers P, Moss C, Carr S, Payo A (2022) Responding to climate change around England's coast - the scale of the transformational challenge. Ocean Coastal Manage 225:106187. https://doi.org/10.1016/j.ocecoaman.2022.106187

Seneviratne SI, Nicholls N, Easterling D Changes in climate extremes and their impacts on the natural physical environment. In: Field CB, Barros V, Stocker, TF Qin D, Dokken DJ, Ebi KL, Mastrandrea MD, Mach KJ, Plattner GK, Allen SK, Tignor M, Midgley PM Managing the risks of extreme events and disasters to advance climate change adaptation: Special Report of the Intergovernmental Panel on Climate Change. Cambridge, UK, and New York, NY, USA: Cambridge University Press:109–230.

Spencer T, Brooks SM, Möller I (2014) Storm-surge impact depends on setting. Nature 505(7481):26–26. https://doi.org/10.1038/505026b

Spencer T, Brooks SM, Evans BR, et al (2015) Southern North Sea storm surge event of 5 December 2013: Water levels, waves and coastal impacts. Earth-Science Rev 146:120–145. https://doi.org/10.1016/j.earscirev.2015.04.002

Steele-Dunne S, Lynch P, McGrath R et al (2008) The impacts of climate change on hydrology in Ireland. J Hydrol 356(1–2):28–45. https://doi.org/10.1016/j.jhydrol.2008.03.025

Surminski S (2021) Business and industry. In: The Third UK Climate Change Risk Assessment Technical Report [Betts, R.A., Haward, A.B. and Pearson, K.V. (eds.)]. Prepared for the Climate Change Committee, London. https://www.ukclimaterisk.org/wp-content/uploads/2021/06/Technical-Report-The-Third-Climate-Change-Risk-Assessment.pdf

Svensson C, Jones DA (2002) Dependence between extreme sea surge, river flow and precipitation in eastern Britain. Int J Climatol 22:1149–1168. https://doi.org/10.1002/joc.794

Swedish Meteorological and Hydrological Institute (2014) HBV – State of the art hydrological modelling. Swedish Meteorological and Hydrological Institute. https://www.smhi.se/polopoly_fs/1.153262!/HBV%20State%20of%20art%20hydrological%20modelling%20190918.pdf. Accessed 3 October 2022

te Linde AH, Aerts JCJH, Hurkmans RTWL, Eberle M (2008) Comparing model performance of two rainfall-runoff models in the Rhine basin using different atmospheric forcing data sets. Hydrol Earth Syst Sci 12(3):943–957. https://doi.org/10.5194/hess-12-943-2008

Teutschbein C, Seibert J (2012) Bias correction of regional climate model simulations for hydrological climate-change impact studies: review and evaluation of different methods. J Hydrol 456–457:12–29. https://doi.org/10.1016/j.jhydrol.2012.05.052

Thumerer T, Jones AP, Brown D (2000) A GIS based coastal management system for climate change associated flood risk assessment on the east coast of England. Int J Geogr Inf Sci 14(3):265–281. https://doi.org/10.1080/136588100240840

UK Marine Monitoring Assessment Strategy (UKMMAS) Community (2010) Charting Progress 2, the state of UK seas. https://tethys.pnnl.gov/sites/default/files/publications/UKMMAS_2010_Charting_Progress_2.pdf. Accessed 19 February 2024

Vozinaki AEK, Morianou GG, Alexakis DD, Tsanis IK (2016) Comparing 1D and combined 1D/2D hydraulic simulations using high-resolution topographic data: a case study of the Koiliaris basin, Greece. Hydrol Sci J 62(4):642–656. https://doi.org/10.1080/02626667.2016.1255746

Wahl T, Jain S, Bender J et al (2015) Increasing risk of compound flooding from storm surge and rainfall for major US cities. Nat Clim Change 5(12):1093–1097. https://doi.org/10.1038/nclimate2736

Wang L, Chen W (2013) Equiratio cumulative distribution function matching as an improvement to the equidistant approach in bias correction of precipitation. Atmospheric Sci Lett 15(1):1–6. https://doi.org/10.1002/asl2.454

Webster T, McGuigan K, Collins K, MacDonald C (2014) Integrated river and coastal hydrodynamic flood risk mapping of the LaHave River Estuary and town of Bridgewater, Nova Scotia. Can Water 6(3):517–546. https://doi.org/10.3390/w6030517

Yin Z, Hu Y, Jenkins K, He Y, Forstenhäusler N, Warren R, Yang L, Jenkins R, Guan D (2021) Assessing the economic impacts of future fluvial flooding in six countries under climate change and socio-economic development. Clim Change 166(3–4). https://doi.org/10.1007/s10584-021-03059-3

Zeiger SJ, Hubbart JA (2021) Measuring and modelling event-based environmental flows: an assessment of HEC-RAS 2D rain-on-grid simulations. J Environ Manage 285:112125. https://doi.org/10.1016/j.jenvman.2021.112125

Zhang X, Lindström G (1996) A comparative study of a Swedish and a Chinese hydrological model. J Am Water Resour Assoc 32(5):985–994. https://doi.org/10.1111/j.1752-1688.1996.tb04067.x